

ThermoBRET: a ligand-engagement nanoscale thermostability assay applied to GPCRs

Bradley L. Hoare^{1,2,\$,&,*}, David N. Tippett^{1,2,#,&}, Amandeep Kaur^{1,2}, Sean A. Cullum^{1,2},
Tamara Miljuš^{1,2,3}, Eline J. Koers^{1,2}, Clare R. Harwood^{1,2}, Nicola Dijon^{1,2}, Nicholas D.
Holliday^{1,2}, David A. Sykes^{1,2,*} and Dmitry B. Veprintsev^{1,2,*}

¹Centre of Membrane Proteins and Receptors (COMPARE), University of Birmingham
and University of Nottingham, Midlands, UK

²Division of Physiology, Pharmacology & Neuroscience, School of Life Sciences,
University of Nottingham, Nottingham, NG7 2UH, UK

³Institute of Metabolism and Systems Research, College of Medical and Dental
Sciences, University of Birmingham, Birmingham B15 2TT, UK

^{\$}Current address: Florey Institute of Neuroscience and Mental Health, The University
of Melbourne, Parkville, VIC 3052, Australia

[#]Current address: Department of Biochemistry, University of Zurich,
Winterthurerstrasse 190, 8057 Zurich, Switzerland

[&]these authors contributed equally

^{*}Correspondence should be addressed to brad.hoare@florey.edu.au,
david.sykes@nottingham.ac.uk and dmitry.veprintsev@nottingham.ac.uk

1 Abstract

2 Measurements of membrane protein thermostability allows indirect detection of ligand
3 binding. Current thermostability assays require protein purification or rely on pre-
4 existing radiolabelled or fluorescent ligands, limiting their application to established
5 target proteins. Alternative methods detect protein aggregation which requires
6 sufficiently high level of protein expression.

7 Here, we present a ThermoBRET method to quantify the relative thermostability of G
8 protein coupled receptors (GPCRs), using cannabinoid receptors (CB₁ and CB₂) and
9 the β_2 -adrenoceptor (β_2 AR) as model systems. ThermoBRET reports receptor
10 unfolding, does not need labelled ligands and can be used with non-purified proteins.
11 It uses Bioluminescence Resonance Energy Transfer (BRET) between
12 Nanoluciferase (Nluc) and a thiol-reactive fluorescent dye that binds cysteines
13 exposed by unfolding. We demonstrate that the melting point (T_m) of Nluc-fused
14 GPCRs can be determined in non-purified detergent solubilised membrane
15 preparations or solubilised whole cells, revealing differences in thermostability for
16 different solubilising conditions and in the presence of stabilising ligands. We extended
17 the range of the assay by developing the thermostable tsNluc by incorporating
18 mutations from the fragments of split-Nluc (T_m of 87 °C vs 59 °C). ThermoBRET allows
19 determination of GPCR thermostability, which is useful for protein purification
20 optimisation and as part of drug discovery screening strategies.

21

22

23

24

25

26

1 Introduction

2 G protein coupled receptors (GPCRs) are a large family of membrane proteins that
3 are important drug discovery targets (Hauser, Attwood et al. 2017). Structural and
4 biophysical studies of GPCRs have significant importance in modern drug discovery
5 (Congreve, de Graaf et al. 2020) but one major hurdle is their successful solubilisation
6 from their native membrane environment and subsequent purification. Optimisation of
7 receptor stability during this process is a key component to success (Tate 2010).
8 Additionally, the ability of a bound ligand to stabilise the receptor structure is a property
9 which can be exploited in screening efforts to find novel drug candidates (Fang 2012,
10 Zhang, Stevens et al. 2015).

11 Existing GPCR protein stability assays rely on the availability of a high-affinity
12 radioligand to act as a tracer for receptor functionality (Galvez, Parmentier et al. 1999,
13 Serrano-Vega, Magnani et al. 2008, Robertson, Jazayeri et al. 2011, Magnani,
14 Serrano-Vega et al. 2016). In the absence of the radioactive tracer, temperature-
15 induced aggregation-based techniques such as technology developed by Heptares
16 Therapeutics (now Sosei Heptares) (Marshall, Jazayeri et al. 2013) or temperature
17 shift fluorescence size exclusion chromatography TS-FSEC (Hattori, Hibbs et al. 2012,
18 Vuckovic 2017, Nji, Chatzikiyriakidou et al. 2018) can be used. Alternative
19 fluorescence-based techniques with higher throughput exist, such as the N-[4-(7-
20 diethylamino-4-methyl-3-coumarinyl)phenyl]maleimide (CPM) assay, which utilises a
21 thiol-reactive fluorescent fluorochrome. This dye reacts with exposed cysteines, acting
22 as a sensor of protein stability in the temperature-dependent unfolding process
23 (Alexandrov, Mileni et al. 2008). Other thiol-reactive dyes such as BODIPY-FL-Cystine
24 (BLC) or 4-(aminosulfonyl)-7-fluoro-2,1,3-benzoxadiazole (ABD) are also available for
25 stability measurements (Isom, Marguet et al. 2011, Bergsdorf, Fiez-Vandal et al.
26 2016). However, both these techniques currently require purified protein in microgram
27 quantities which is a considerable drawback.

28 Low abundance of GPCRs even in over-expressing systems and their inherently low
29 stability in detergents (Milic and Vepintsev 2015) calls for sensitive protein stability
30 assays that can be used without protein purification or pre-existing tracer compounds.

31 Here, we present the ThermoBRET assay based on bioluminescence resonance
32 energy transfer between the bright Nanoluciferase (Nluc, and, correspondingly,
33 NanoBRET) (Hall, Unch et al. 2012), acting as a donor of light and a thiol reactive
34 Sulfo-Cyanine3 maleimide (SCM) dye, the acceptor, allowing us to quantify the relative
35 thermostability of non-purified GPCRs solubilised into detergent micelles. As a test
36 case we focus on two GPCRs, the cannabinoid receptor 2 (CB₂) as a therapeutically
37 promising (Pertwee 2012) but unstable drug target (Vukoti, Kimura et al. 2012,
38 Beckner, Gawrisch et al. 2019, Beckner, Zoubak et al. 2020) and the previously well
39 characterised β_2 adrenergic (β_2 AR) receptor. This assay detects picomolar
40 concentration, corresponding to nanogram amounts, of target protein. Due to the
41 nature of the homogeneous assay format, negating the need to separate bound and

1 unbound ligand, can be used to detect binding of low-affinity ligands. Since we employ
2 NanoBRET detection, these assays are safer than radiometric alternatives and can be
3 readily performed in 96- and 384-well assay format.

4

5 Results

6 *ThermoBRET provides reliable measurements of GPCR stability*

7 We fused a Nluc (Hall, Unch et al. 2012) to the receptor N-terminus, preceded by a
8 cleaved signal peptide to ensure its' successful expression and plasma membrane
9 trafficking ([Supplementary Information 1](#)). Detergent solubilised receptor samples
10 containing a thiol reactive Sulfo-Cyanine3 maleimide (SCM) acceptor are incubated at
11 varying temperatures using a gradient forming PCR thermocycler. As the receptor
12 unfolds on heating the SCM covalently binds to exposed cysteine residues ([Figure 1](#)).
13 We chose SCM because of its suitability as a BRET acceptor for Nluc, water solubility,
14 and relatively low cost compared to other thiol-reactive fluorophores. In principle, any
15 maleimide or other thiol-reactive conjugated fluorescent dye with overlapping donor-
16 acceptor emission-absorption spectra can be used. The unfolded state of the receptor
17 due to thermal denaturation is measured as NanoBRET between the Nluc tag and the
18 SCM acceptor and is quantified as a ratio of the donor and acceptor light emissions,
19 termed the NanoBRET ratio. The relative thermostability of a receptor in different
20 solubilised non-purified membrane preparations can be easily determined, first by
21 thermal denaturation across a temperature gradient on a thermocycler block, rapid
22 cooling to 4 °C, and then following the addition of the Nluc substrate furimazine and
23 measurement of the NanoBRET ratio in a 384-well luminescence plate reader at room
24 temperature ([Figure 1](#)). The midpoint of the transition curve is found by fitting the data
25 to a Boltzmann sigmoidal equation to obtain a T_m .

26 *Detergents affect stability of receptors*

27 When solubilised in DDM detergent, CB₂ had a T_m of around 33 °C ([Figure 2A](#)) and
28 was marginally more stable in LMNG ($T_m = 35$ °C). Addition of CHAPSO and the
29 cholesterol derivative CHS in the detergent micelles provided the highest
30 thermostability for CB₂ ($T_m = 43$ °C in LMNG/CHAPSO/CHS). This observation is
31 consistent with the reported increase in CB₂ stability in DDM/CHAPSO mixed micelles
32 (Vukoti, Kimura et al. 2012).

33 Differences in the detergent stability of the adrenergic β_2 -receptor were also found
34 ([Supplementary Figure 1](#)). Hence, this assay can be readily used to screen for the
35 best detergent solubilising conditions before attempting a large-scale purification.

36 *Ligands stabilise CB₂*

37 We also tested a selection of endogenous and synthetic cannabinoid receptor ligands
38 for their ability to increase the thermostability of CB₂ ([Figure 2B](#)). The lipophilicity of its

1 ligands has made the CB₂ receptor a particularly challenging target for ligand binding
2 experiments due to their high non-specific binding. These ligands were all tested at a
3 concentration of 20 μM, well above their dissociation constant (K_D) at room
4 temperature, in order to ensure full occupancy of the solubilised receptors.
5 Interestingly, the endogenous cannabinoid 2-arachidonoylglycerol (2AG) increased
6 the T_m of CB₂ by around 6 °C, whereas the other endogenous cannabinoid
7 anandamide (AEA) only increased the T_m by around 2 °C. The most probable reason
8 for these observations are the variable temperature dependence of the affinity of the
9 ligand to the receptor as well as well as the degree of the entropy contribution to the
10 binding (Layton and Hellinga 2010). Other synthetic cannabinoid ligands HU308 and
11 SR144528 also produced appreciable increases in thermostability, and the pattern of
12 ligand stabilisation appeared different for the related CB₁ receptor ([Supplementary](#)
13 [Figure 2](#)).

14 *tsNluc extends the range of the ThermoBRET assay*

15 One problematic aspect of the ThermoBRET is the thermostability of the Nluc donor
16 itself, which has been reported to unfold at around 55 - 60 °C (Hall, Unch et al. 2012).
17 This limits the thermal range for this assay and prevents accurate T_m determination in
18 conditions where the receptor itself is particularly thermostable, for example when CB₂
19 is bound to the high affinity non-selective cannabinoid agonist HU210 ([Figure 2C](#)). We
20 therefore combined Nluc mutations which had been developed by Promega as part of
21 their efforts to create a stable split-luciferase system (Dixon, Schwinn et al. 2016) and
22 found that these mutations improved thermostability of the full length luciferase by
23 about 30 °C ([Figure 2D](#)). In line with previous reports (Hall, Unch et al. 2012) we found
24 that purified Nluc had a T_m of 59 °C, and that purified thermostable Nluc (tsNluc) had
25 a T_m of 87 °C ([Figure 2D](#)), making it preferable for thermostability measurements
26 across a wide temperature range. Importantly, tsNluc contains no cysteine residues
27 ([Supplementary Information 2](#)) and thus is unaffected by maleimide/thiol chemistry.
28 Further characterisation showed tsNluc to have a similar luminescence emission
29 profile as Nluc with furimazine as a substrate, although with a lower luminescence
30 output ([Supplementary Figure 3](#)). Applying this novel tsNluc fusion improved the
31 working temperature range of the ThermoBRET assay and allowed successful T_m
32 determination for CB₂ in the presence of HU210 ([Figure 2E](#)). Strikingly, HU210 was
33 able to stabilise CB₂ by around 12 °C, the highest level achieved of any of the CB₂
34 ligands tested.

35 To further assess the ability of this improved assay format to determine the stability of
36 GPCRs in detergent we created a tsNluc-β₂AR expression construct. Previous work
37 employing the CPM assay indicates that this receptor can be stabilised by high affinity
38 antagonists ([Wacker, Fenalti et al. 2010](#)). Due to the higher throughput achievable
39 with our BRET-based system we were able to assess the receptor stabilising effects
40 of both β-adrenergic agonists and antagonists ([Figure 3 A and B](#)). Both high affinity
41 antagonist and agonist were able to stabilise the receptor to a degree which was
42 dependent on the affinity of the ligands for the receptor ([Figure 3C](#)). In contrast k_{off} and

1 k_{on} were by themselves more poorly correlated with receptor stabilisation (Figure 3D
2 and E).

3 *Lipid concentration in lipid-detergent micelles affects stability of the receptor*

4 Having established a robust assay to measure receptor stability, we examined the
5 more subtle effects of lipid-detergent ratio in the solubilised tsNluc-CB₂. Firstly, we
6 examined if the stability of CB₂ is affected by the receptor concentration, while keeping
7 the membrane fraction/detergent ratio the same by supplementing the fraction of CB₂
8 membranes with “empty” non-transfected HEK293 membranes to the same total
9 amount (Supplementary Figure 4A). The reported value was the same, suggesting
10 that CB₂ stability is not affected by its concentration, at least within the tested range.
11 Secondly, we examined if an increase in membrane/detergent ratio could affect CB₂
12 stability, by supplementing a fixed amount of CB₂ membranes with an increasing
13 amount of “empty” membranes (Supplementary Figure 4B). Surprisingly, the receptor
14 stability was decreased by 2-3 °C at higher membrane/detergent ratio, although it
15 plateaued at concentrations above 20 ng/μL, as generally increasing concentration of
16 lipids may lead to stabilisation of receptors (Cecchetti, Strauss et al. 2021). A possible
17 explanation for this is that the increased total protein concentration (HEK293
18 membranes contain a significant amount of protein) may accelerate aggregation
19 process. This observation suggests that for each new target this relationship needs to
20 be explored, and concentration of membrane and detergent should be kept constant
21 and an appropriate point on the plateau region should be chosen.

22 *Stability of the receptor measured by ThermoBRET reflects a loss of ligand binding*

23 Receptor denaturation is a complex process, progressing through a loss of tertiary
24 structure through potential intermediates that may have the overall organisation of the
25 correctly folded receptor (and protecting cysteines from modification) to complete loss
26 of tertiary structure and aggregation. It is important to understand what process is
27 sensed by the ThermoBRET assay.

28 Stabilisation of a receptor can also be monitored through addition of a fluorescent
29 ligand to a detergent solubilized receptor, measured using NanoBRET detection. In
30 this case unfolding of a target protein in response to an increase in temperature will
31 result in a loss in specific binding. Figure 4A shows the saturation binding curve for
32 propranolol-green binding to the tsNluc-β₂AR receptor solubilised in DDM. The K_d of
33 propranolol-green for the β₂AR was determined to be 5.7 ± 1.1 nM. Figure 4B shows
34 the loss in propranolol-green specific binding signal as the protein unfolds in response
35 to an increase in temperature, following preincubation of a saturating concentration of
36 fluorescent ligand (1 μM) with the receptor.

37 *Isothermal ThermoBRET*

38 Finally, we assessed the dependency of agonist and antagonist ligand concentration
39 on tsNluc-β₂AR thermostability at a constant temperature 35°C, just above the T_m of
40 the apo form of the receptor. Receptor stability measurements expressed as a

1 function of ligand concentration are shown in [Figure 5A](#). ThermoBRET IC₅₀ values
2 were derived for this smaller test set and correlated with the thermal shift values
3 obtained at fixed concentrations of individual agonist and antagonists. A linear
4 relationship was observed between these two measures ([Figure 5B](#)). Finally, the
5 ThermoBRET IC₅₀ values were correlated with radioligand binding affinity values
6 obtained for the different ligands ([Figure 5C](#)). Again, an excellent correlation was
7 observed between the two data sets apart from for the very slowly dissociating
8 antagonist cyanopindolol. There are two plausible explanations for this: either the very
9 slow off-rate of this ligand means that for this ligand equilibrium is not achieved prior
10 to the determination of ThermoBRET IC₅₀ values, samples being kept on ice prior to
11 melting, or we are observing the phenomenon of ligand depletion due to nM
12 concentrations of receptor present in the reaction mixture.

13 *Assay sensitivity*

14 Solubilised receptor concentration was estimated by extrapolation from a standard
15 curve of the luminescence emission from purified tsNluc protein of known
16 concentrations. ThermoBRET assay sensitivity was then determined by dilution of this
17 solubilized β_2 AR receptor sample with receptor stabilisation assessed by monitoring
18 the change in BRET ratio as a function of increasing temperature, see [Supplementary](#)
19 [Figure 5](#). This confirms that ThermoBRET is a nanoscale system with sensitivity in line
20 with that of a traditional ligand binding assay. In further experiments we tested the
21 effect of SCM dye concentration on the thermal unfolding of the β_2 AR (see
22 [Supplementary Figure 6](#)), confirming that dye concentrations in the region of 1-3 μ M
23 are sufficient to monitor the unfolding of GPCRs and without significant quenching of
24 the luminescent signal.

25 *Receptor solubilisation directly from cells*

26 In addition, we assessed the stability of the β_2 AR solubilised directly from whole cells
27 and the ability of orthosteric ligands to stabilise the receptor. [Figure 6](#) shows the
28 measured stability of the apo β_2 AR solubilised from whole cells in the absence and
29 presence of a selection of antagonist and agonist ligands and the resulting correlation
30 of T_m values obtained with the same ligands from membrane solubilised receptors.
31 The measurement of receptor thermostability directly from whole cells further reduces
32 the number of steps required for the assay (ie. no need to prepare membranes) and
33 allows target engagement to be assayed when receptors are still in a native membrane
34 environment if it is added prior to solubilisation.

35 Discussion

36 Here, we aimed to establish sensitive technique that allows to measure receptor
37 stability in crude detergent-solubilised preparations, without a need for a unique tracer
38 compound. ThermoBRET proved to be sensitive and selectively reporting protein
39 stability of solubilised membrane preparations and even directly solubilised cells. It

1 utilises universal cysteine-reactive fluorescent dyes for readout and can be used to
2 detect binding of specific non-fluorescent ligands.

3 The processes of protein unfolding and protein aggregation are related, yet very
4 separate, phenomena. As mentioned in the introduction, a decrease in GFP
5 fluorescence (Vuckovic 2017, Nji, Chatzikyriakidou et al. 2018) or luciferase signal
6 (Marshall, Jazayeri et al. 2013) has been used for measuring temperature-induced
7 aggregation of GPCRs. Nluc has also been successfully used in similar applications
8 which monitor protein aggregation of soluble proteins. Such applications fuse either
9 full length Nluc (Dart, Machleidt et al. 2018) or split Nluc (Martinez, Asawa et al. 2018)
10 to the protein of interest and monitor the decrease in luminescence activity to measure
11 aggregation of the protein of interest after thermal denaturation. In contrast, the
12 ThermoBRET assay described here captures the initial conformational unfolding
13 events which expose maleimide reactive cysteine residues in the protein of interest.
14 In addition, ThermoBRET measurement is buffered from changes in the concentration
15 of the luciferase fused target protein because a ratiometric method is used to calculate
16 resonance energy transfer, contrasting with assays which measure luminescence
17 intensity only. This means the measurement remains robust even at low
18 concentrations of the target protein where the magnitude of the measured signal is at
19 the lower end of detection capabilities.

20 We note that under the test conditions used, the luminescence activity of just 85 pM
21 purified Nluc and tsNluc was measurable in a 96-well plate (Figure 2D), making the
22 assay extremely sensitive. This makes the assay particularly amenable situations
23 where there are limitations on the amounts of reagent that can be provided, for
24 example protein targets which are poorly expressed *in vitro* and/or *in vivo*. This assay
25 principle could even be applied in more physiologically relevant *in vivo* cellular models
26 whereby tsNluc (or the 11 amino acid HiBiT tag) is fused to an endogenously
27 expressed protein via CRISPR-mediated insertion (White, Johnstone et al. 2019).

28 The novel thermostable tsNluc we describe has clear advantages compared to Nluc.
29 Firstly, due to its improved thermostability it is less likely to unfold before the protein
30 of interest and cause sample aggregation and other possible artefacts. The T_m of
31 tsNluc was 87 °C which may put an upper temperature limit on the ThermoBRET
32 method, however such a high thermostability situation would be very unexpected for
33 an integral membrane protein solubilised in detergents. Secondly, whilst previous
34 reports (Hall, Unch et al. 2012) and our own data (Figure 2D) showed the T_m of Nluc
35 to be 59 °C, more recent use of Nluc to monitor protein aggregation show clear
36 luminescence activity after protein samples had been heated to temperatures >60 °C
37 before cooling (Dart, Machleidt et al. 2018). We speculate that Nluc has propensity to
38 spontaneously refold after thermal denaturation, and that the presence of detergents
39 in the buffers of the latter report either aided Nluc refolding or delayed irreversible
40 protein aggregation. In our ThermoBRET assays, the cysteine exposed upon Nluc
41 unfolding would potentially react with the SCM and prevent its refolding, whereas
42 tsNluc avoids these pitfalls. The cysteine-less sequence of tsNluc also allows easy *in*

1 *vitro* chemical tagging of tsNluc-fusions. There is of interest in producing conjugates
2 of Nluc fused to other biomolecules, though usually this involves incorporation of
3 sequence-specific ligation motifs onto Nluc followed by enzyme-mediated ligation to
4 the molecule of interest (Wang, Shao et al. 2017, Mie, Niimi et al. 2019, Wouters, Vugs
5 et al. 2020). By introducing a cysteine at the C-terminus of tsNluc, any molecule could
6 be conjugated to tsNluc by thiol-reactive chemistry and mild reaction conditions,
7 enhancing its potential for protein engineering and enabling a wide scope for future
8 applications.

9 In comparison to our previous ThermoFRET application using a terbium cryptate
10 labelled receptor as a FRET donor (Tippett, Hoare et al. 2020), the ThermoBRET
11 approach offers potential advantages. ThermoFRET requires cell surface labelling of
12 the receptor-fused SNAP tag with the terbium cryptate donor molecule, adding to
13 assay cost, but perhaps more importantly creating an extra labelling step that can be
14 problematic if the tag is not readily exposed at the plasma membrane. In contrast, the
15 use of a genetically encoded bioluminescent donor (ie. tsNluc or Nluc) omits this
16 labelling step. This means that fused proteins which are poorly trafficked to the plasma
17 membrane, are now amenable as they do not require labelling at the cell surface.
18 Additionally, ThermoFRET requires more sophisticated detection by plate readers with
19 time-resolved fluorescence detection capabilities, whereas BRET only requires a
20 luminometer with filtered light detection that are more readily available in many labs.
21 A comparison of biophysical techniques used in drug screening cascades is shown in
22 [Figure 7](#) along with the relative protein requirements and assay throughput potential
23 of each technique.

24 The ability of the ThermoBRET assay to quantify ligand-induced changes in the
25 receptor T_m makes it an ideal tool to study ligand binding to GPCRs. T_m values
26 obtained in the current study for the β_2 AR specific ligands compare well with those
27 obtained previously (Zhang et al., 2015). In principle, this assay can detect compounds
28 which bind the target at any site, assuming this interaction influences the
29 thermodynamic conformational landscape of the protein. It can be used to screen
30 potential ligands for orphan GPCRs as it does not depend on the availability of tool
31 compounds or known binders to develop a competition assay. Moreover, it could be
32 used to detect the combined stabilisation of several ligands to discover positive and
33 negative allosteric modulators of GPCRs.

34 Despite a number of advantages ThermoBRET offers, and positive results obtained
35 for β_2 AR, CB₂ and CB₁ receptors, this technique is not immune to the general
36 limitations of thermal shift assays. The protein needs to be in a native state once
37 solubilised, and some condition optimisation may need to be done for the less stable
38 receptors. Correspondingly, it may not be successful for every target receptor tried as
39 there is a requirement that the receptor contains buried cysteines which become
40 exposed upon thermal denaturation. This limitation is also inherent for the CPM assay,
41 and in situations where no free thiol exists then cysteines could be rationally
42 introduced into the receptor sequence to generate a ThermoBRET signal. Finally, more

1 practical experience with screening larger compound libraries will be needed to
2 establish real life performance and limitations of this technique.

3 Overall, ThermoBRET is an excellent and highly sensitive tool for optimisation of
4 solubilisation conditions and biophysical screening of GPCR compound libraries to
5 support structural biology, aiding the drug discovery efforts.

6 Methods

7 *Drug compounds and reagents*

8 Sulfo-Cy3 maleimide (SCM) (Lumiprobe GmbH, Germany) was obtained in powder
9 form, dissolved in DMSO at a concentration of 10 mM and stored in the dark at -20C.
10 Furimazine, the substrate for Nluc, was obtained from the Nano-Glo Luciferase Assay
11 System kit (Promega, UK) provided at a concentration of 5 mM. Cannabinoid ligands
12 (anandamide [AEA], 2-arachydonyl-glycerol [2AG], SR144528, HU210, HU308,
13 cannabiniol) were obtained from Tocris Bioscience and dissolved in DMSO to a storage
14 concentration of 10 mM, except AEA and 2AG which were dissolved in EtOH.
15 Rimonabant was obtained from Roche Pharmaceuticals GmbH (Germany).

16 *Plasmid construction*

17 For mammalian cell expression, receptor constructs were cloned into pcDNA4/TO
18 using Gibson assembly (Gibson, Young et al. 2009). All GPCR constructs contained
19 an N-terminal signal peptide (which is cleaved by signal peptidases during protein
20 maturation and trafficking) to improve expression, followed by a TwinStrep affinity tag,
21 then Nluc (or tsNluc) followed by the receptor sequence. The TwinStrep affinity tag
22 was not required for these studies but was present to facilitate receptor purification
23 and antibody-based detection if required. The synthesized cDNA for tsNluc was
24 obtained from GeneArt Gene synthesis (Invitrogen). For bacterial cell expression of
25 Nluc and tsNluc, cDNA sequences were cloned into the pJ411 expression plasmid
26 with a N-terminal 10X histidine affinity tag and TEV cleavage site encoded upstream
27 of the protein of interest. Amino acid sequences of the constructs used are provided
28 in [Supplementary Information 1](#). The correct sequence within the expression cassette
29 of all plasmid constructs was verified by Sanger sequencing (Genewiz, UK).

30 *Mammalian cell culture*

31 The T-RexTM-293 cell line (HEK293TR; ThermoFisher Scientific) was used to make
32 stable expressing cell lines for receptors cloned into pcDNA4/TO. HEK293TR cells
33 were cultured in growth medium (DMEM, 10% FCS, 5 µg/mL blasticidin) in a 37 °C
34 humidified incubator with 5% CO₂. Stable cell lines were generated by PEI transfection
35 of pcDNA4/TO plasmids into HEK293TR cells. 24-48 hours after transfection, 20
36 µg/mL zeocin was incorporated into the growth medium until stable expressing,
37 zeocin-resistant cell populations remained (2-4 weeks). To produce cells for
38 membrane preparations, 1X T175 culture flask of confluent stable cells were treated
39 with 1 µg/mL tetracycline for 48h to induce receptor expression. Following this, cells

1 were lifted by trituration and centrifuged at 500 g for 10 minutes. Cell pellets were then
2 frozen at -80 °C until membranes were prepared.

3 *Membrane preparations*

4 HEK293TR cell pellets were resuspended in 20 mL of ice cold buffer (10 mM HEPES
5 pH 7.4, 10 mM EDTA) and homogenised using a Ultra Turrax (Ika Work GmbH,
6 Germany). The homogenised cell suspension was then centrifuged at 4 °C for 5
7 minutes at 500 g to remove whole cells and large debris, and the remaining
8 supernatant was then centrifuged twice at 4 °C and 48,000 g for 30 minutes before the
9 membrane pellet was resuspended in buffer (10 mM HEPES pH 7.4, 0.1 mM EDTA).
10 Protein concentration of resuspended membranes was determined with using Pierce
11 BCA Protein assay kit (ThermoFisher Scientific) and was adjusted to 3 – 10 mg/mL
12 before being aliquoted and stored at -80 °C.

13 *ThermoBRET experiments*

14 The CORE buffer for thermostability experiments contained 20 mM HEPES pH 7.5,
15 150 mM NaCl, 10% w/v glycerol, 0.5% w/v BSA. Cell membranes were diluted in
16 CORE buffer to approximately 0.1 – 0.5 mg/mL total protein and were then centrifuged
17 at 16,000 g for 60 minutes at 4 °C to remove residual EDTA from the membrane
18 preparation buffers. Membrane pellets were then resuspended in CORE buffer
19 containing detergent, and samples were incubated at 4 °C with gentle shaking for 1h
20 to solubilise membranes. Detergent/CHS concentrations used were either 1% DDM,
21 1% DDM / 0.5 % CHAPSO / 0.3% CHS, 0.5% LMNG, or 0.5% LMNG / 0.5% CHAPSO
22 / 0.3% CHS. Samples were then centrifuged again at 16,000 g for 60 minutes at 4 °C
23 to remove unsolubilised material, and the resulting supernatant containing detergent
24 micelles was transferred to a fresh tube. These supernatants were then kept on ice for
25 up to 48 hours during testing. For thermostability testing, solubilised receptors were
26 diluted 10-fold in CORE buffer with the addition of 1 µM SCM and 20 µM of ligand (if
27 used). This was incubated on ice for 15 minutes before being aliquoted across 96-well
28 PCR plates and placed in the pre-cooled (4 °C) PCRmax Alpha Cyclor 2 Thermal
29 Cyclor (Cole-Palmer Ltd, St. Neots, UK). Samples were then incubated at different
30 temperatures for 30 minutes via a temperature gradient across the plate. Following
31 rapid cooling of the samples to 4 °C, samples were then transferred to white 384-well
32 proxiplates (Perkin Elmer) containing furimazine at a final concentration of 10 µM. The
33 plate was then read using a PHERAstar FSX plate reader (BMG) at room temperature
34 and the 450BP80/550LP filter module. Measurements were performed in singlet for
35 each temperature point. Whole cell experiments (10 million cells/mL of 1% DDM)
36 were performed essentially as described above but receptor solubilisation was
37 performed in the presence of protease inhibitor cocktail (cComplete™ mini EDTA-free
38 Protease Inhibitor cocktail (Roche)).

1 *Nluc and tsNluc expression and purification*

2 NiCo21(DE3) chemically competent E. coli were transformed with pJ411 bacterial
3 expression plasmids and plated onto LB/agar plates containing 2% w/v glucose and
4 50 µg/mL kanamycin. After incubation at 37 °C for 16-24 hours, a single colony was
5 picked to inoculate 20 mL of terrific broth containing 0.2% w/v glucose and 50 µg/mL
6 kanamycin. After 16-24 hours in a shaking incubator set at 37 °C, 15 mL of overnight
7 culture was added to 3 L of terrific broth containing 0.2% w/v glucose and 50 µg/mL
8 kanamycin, grown in a shaking incubator at 37 °C until OD₆₀₀ of 0.7-1, when 500 µM
9 of isopropyl-β-D-thiogalactopyranoside (IPTG; VWR Chemicals) was added to induce
10 protein expression. Cells were then grown overnight (16-20 hours) at 25 °C in a
11 shaking incubator before being harvested by centrifugation and frozen at -80 °C. Cell
12 pellets were then thawed on ice, and resuspended in 100 mL lysis buffer (100 mM Tris
13 pH 7.5, 300 mM NaCl, 0.25 mg/mL chicken lysozyme, 1 µg/mL bovine DNase I, 4 mM
14 MgCl₂, and 3 cOmplete™ mini EDTA-free Protease Inhibitor cocktail tablets (Roche)).
15 After 1h on ice in lysis buffer, cells were then lysed further by French press. Cell lysates
16 were then clarified by centrifugation at 25,000 rcf for 30 minutes and then by passing
17 through a 0.45 µm syringe filter. The His-tagged proteins from the resulting lysate were
18 then purified using a 5mL HiTrap TALON Crude column on an ÄKTA start protein
19 purification system (Cytiva Life Sciences) and eluted with 150 mM imidazole. Elution
20 fractions were analysed by SDS-PAGE and fractions which contained no visible
21 contaminants proteins were pooled together. Protein concentration was determined
22 by A₂₈₀ measurement on a Denovix DS-11 FX series spectrophotometer assuming the
23 calculated molar extinction coefficient (ϵ_{280}) of 26,930 mol⁻¹.cm⁻¹ for both proteins.

24 *Luminescence activity thermostability experiments*

25 Purified Nluc and tsNluc proteins were serially diluted from around 200 µM down to
26 100 pM in CORE buffer. Proteins were then aliquoted across 96-well PCR plates (100
27 µL per well) and placed in the pre-cooled (4 °C) PCRmax Alpha Cyclor 2 Thermal
28 Cyclor (Cole-Palmer Ltd, St. Neots, UK). Samples were then incubated at different
29 temperatures for 30 minutes via a temperature gradient across the plate. Following
30 rapid cooling to 4 °C, 85 µL of samples were then transferred to white 96 well plates
31 (Perkin Elmer) containing 15 µL of diluted furimazine to a final concentration of 10 µM.
32 After 30 seconds of gentle shaking, the luminescence intensity was measured in a
33 PHERAstar FSX plate reader at room temperature. Measurements were performed in
34 triplicate for each temperature point, and three independent experiments were
35 performed.

36 *Curve fitting and data analysis*

37 All curve fitting and data manipulation was performed using GraphPad Prism 8. For
38 ThermoBRET measurements, NanoBRET ratio was defined as the 550LP emission
39 divided by the 450BP80 emission. In situations in which the NanoBRET ratio
40 decreased at high temperatures (presumably due to protein aggregation and loss of
41 signal), the data was manually truncated after the highest point. Data was then

1 normalised to the upper (100%) and lower (0%) datapoints and fitted using a
2 Boltzmann sigmoidal equation constrained to upper and lower values of 0% and 100%.
3 For luminescence thermostability measurements, unfiltered luminescence was
4 normalised to the top point of the dataset and fitted using a Boltzmann sigmoidal
5 equation with no constraints.

6 Data availability statement

7 All data used to support the conclusions are included in the paper. Raw numerical data
8 can be obtained by contacting the corresponding authors.

9 Acknowledgements

10 AK was funded by a COMPARE team science summer studentship (2019) awarded
11 to BH. This research was supported by COMPARE funding to DBV. We would like to
12 thank Uwe Grether for supplying the CB₁ antagonist rimonabant.

13 Declaration of interests

14 D.A.S and D.B.V are founders and directors of Z7 Biotech Ltd, an early-stage drug
15 discovery contract research company. All other authors declare no conflict of interest.

16

17 References

18 Alexandrov, A. I., M. Mileni, E. Y. Chien, M. A. Hanson and R. C. Stevens (2008).
19 "Microscale fluorescent thermal stability assay for membrane proteins." *Structure*
20 16(3): 351-359.

21 Beckner, R. L., K. Gawrisch and A. Yeliseev (2019). "Radioligand Thermostability
22 Assessment of Agonist-Bound Human Type 2 Cannabinoid Receptor." *Biophysical*
23 *Journal* 116(3): 193a.

24 Beckner, R. L., L. Zoubak, K. G. Hines, K. Gawrisch and A. A. Yeliseev (2020).
25 "Probing thermostability of detergent-solubilized CB₂ receptor by parallel G protein-
26 activation and ligand-binding assays." *Journal of Biological Chemistry* 295(1): 181-
27 190.

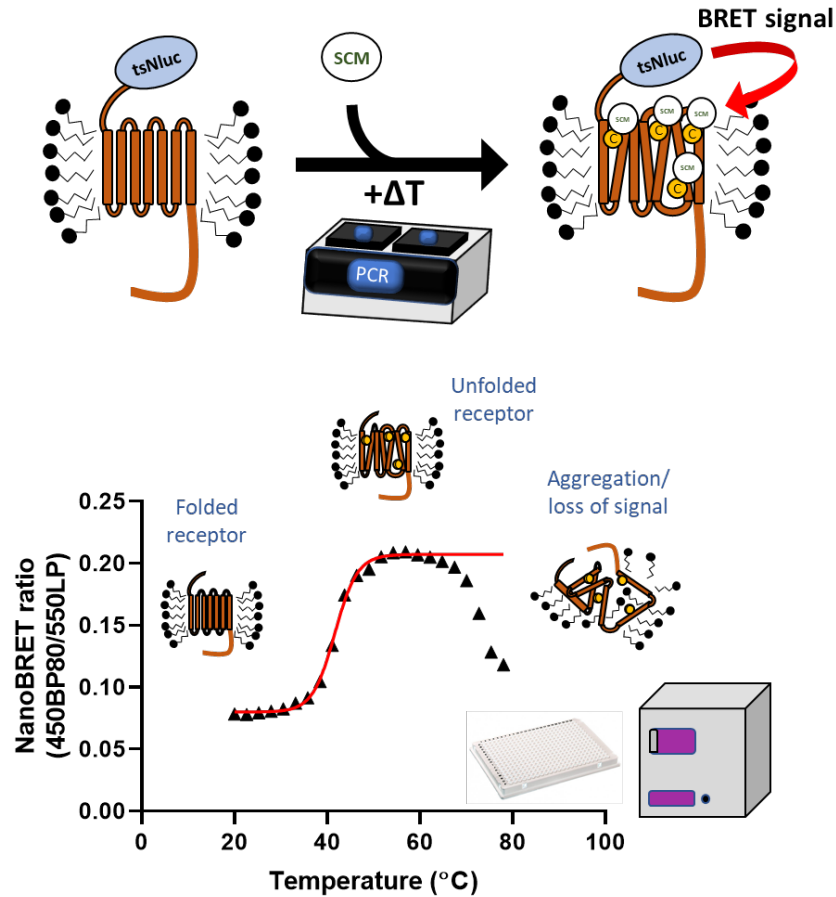
28 Bergsdorf, C., C. Fiez-Vandal, D. A. Sykes, P. Bernet, S. Aussenac, S. J. Charlton, U.
29 Schopfer, J. Ottl and M. Duckely (2016). "An Alternative Thiol-Reactive Dye to Analyze
30 Ligand Interactions with the Chemokine Receptor CXCR2 Using a New Thermal Shift
31 Assay Format." *J Biomol Screen* 21(3): 243-251.

32 Cecchetti, C., J. Strauss, C. Stohrer, C. Naylor, E. Pryor, J. Hobbs, S. Tanley, A.
33 Goldman and B. Byrne (2021). "A novel high-throughput screen for identifying lipids
34 that stabilise membrane proteins in detergent based solution." *PLoS One* 16(7):
35 e0254118.

- 1 Congreve, M., C. de Graaf, N. A. Swain and C. G. Tate (2020). "Impact of GPCR
2 structures on drug discovery." *Cell* 181(1): 81-91.
- 3 Dart, M. L., T. Machleidt, E. Jost, M. K. Schwinn, M. B. Robers, C. Shi, T. A. Kirkland,
4 M. P. Killoran, J. M. Wilkinson, J. R. Hartnett, K. Zimmerman and K. V. Wood (2018).
5 "Homogeneous Assay for Target Engagement Utilizing Bioluminescent Thermal Shift."
6 *ACS Medicinal Chemistry Letters* 9(6): 546-551.
- 7 Dixon, A. S., M. K. Schwinn, M. P. Hall, K. Zimmerman, P. Otto, T. H. Lubben, B. L.
8 Butler, B. F. Binkowski, T. Machleidt and T. A. Kirkland (2016). "NanoLuc
9 complementation reporter optimized for accurate measurement of protein interactions
10 in cells." *ACS chemical biology* 11(2): 400-408.
- 11 Fang, Y. (2012). "Ligand–receptor interaction platforms and their applications for drug
12 discovery." *Expert opinion on drug discovery* 7(10): 969-988.
- 13 Galvez, T., M.-L. Parmentier, C. Joly, B. Malitschek, K. Kaupmann, R. Kuhn, H.
14 Bittiger, W. Froestl, B. Bettler and J.-P. Pin (1999). "Mutagenesis and Modeling of the
15 GABAB Receptor Extracellular Domain Support a Venus Flytrap Mechanism for
16 Ligand Binding." *Journal of Biological Chemistry* 274(19): 13362-13369.
- 17 Gibson, D. G., L. Young, R.-Y. Chuang, J. C. Venter, C. A. Hutchison and H. O. Smith
18 (2009). "Enzymatic assembly of DNA molecules up to several hundred kilobases."
19 *Nature methods* 6(5): 343-345.
- 20 Hall, M. P., J. Unch, B. F. Binkowski, M. P. Valley, B. L. Butler, M. G. Wood, P. Otto,
21 K. Zimmerman, G. Vidugiris and T. Machleidt (2012). "Engineered luciferase reporter
22 from a deep sea shrimp utilizing a novel imidazopyrazinone substrate." *ACS chemical
23 biology* 7(11): 1848.
- 24 Hall, M. P., J. Unch, B. F. Binkowski, M. P. Valley, B. L. Butler, M. G. Wood, P. Otto,
25 K. Zimmerman, G. Vidugiris, T. Machleidt, M. B. Robers, H. A. Benink, C. T. Eggers,
26 M. R. Slater, P. L. Meisenheimer, D. H. Klaubert, F. Fan, L. P. Encell and K. V. Wood
27 (2012). "Engineered luciferase reporter from a deep sea shrimp utilizing a novel
28 imidazopyrazinone substrate." *ACS Chem Biol* 7(11): 1848-1857.
- 29 Hattori, M., R. E. Hibbs and E. Gouaux (2012). "A fluorescence-detection size-
30 exclusion chromatography-based thermostability assay for membrane protein
31 precrystallization screening." *Structure* 20(8): 1293-1299.
- 32 Hauser, A. S., M. M. Attwood, M. Rask-Andersen, H. B. Schioth and D. E. Gloriam
33 (2017). "Trends in GPCR drug discovery: new agents, targets and indications." *Nat
34 Rev Drug Discov* 16(12): 829-842.
- 35 Isom, D. G., P. R. Marguet, T. G. Oas and H. W. Hellinga (2011). "A miniaturized
36 technique for assessing protein thermodynamics and function using fast determination
37 of quantitative cysteine reactivity." *Proteins* 79(4): 1034-1047.

- 1 Layton, C. J. and H. W. Hellinga (2010). "Thermodynamic Analysis of Ligand-Induced
2 Changes in Protein Thermal Unfolding Applied to High-Throughput Determination of
3 Ligand Affinities with Extrinsic Fluorescent Dyes." *Biochemistry* 49(51): 10831-10841.
- 4 Magnani, F., M. J. Serrano-Vega, Y. Shibata, S. Abdul-Hussein, G. Lebon, J. Miller-
5 Gallacher, A. Singhal, A. Strege, J. A. Thomas and C. G. Tate (2016). "A mutagenesis
6 and screening strategy to generate optimally thermostabilized membrane proteins for
7 structural studies." *Nat Protoc* 11(8): 1554-1571.
- 8 Marshall, F. H., A. Jazayeri and J. C. Patel (2013). WO 2013/179062. Assays for
9 assessing the stability of a membrane protein, especially a G protein-coupled receptor
10 (GPCR). . WO, HEPTARES THERAPEUTICS LTD.
- 11 Martinez, N. J., R. R. Asawa, M. G. Cyr, A. Zakharov, D. J. Urban, J. S. Roth, E.
12 Wallgren, C. Klumpp-Thomas, N. P. Coussens and G. Rai (2018). "A widely-applicable
13 high-throughput cellular thermal shift assay (CETSA) using split Nano Luciferase."
14 *Scientific reports* 8(1): 1-16.
- 15 Mie, M., T. Niimi, Y. Mashimo and E. Kobatake (2019). "Construction of DNA-NanoLuc
16 luciferase conjugates for DNA aptamer-based sandwich assay using Rep protein."
17 *Biotechnology Letters* 41(3): 357-362.
- 18 Milic, D. and D. B. Veprintsev (2015). "Large-scale production and protein engineering
19 of G protein-coupled receptors for structural studies." *Front Pharmacol* 6: 66.
- 20 Nji, E., Y. Chatzikiyriakidou, M. Landreh and D. Drew (2018). "An engineered thermal-
21 shift screen reveals specific lipid preferences of eukaryotic and prokaryotic membrane
22 proteins." *Nature Communications* 9(1).
- 23 Pertwee, R. G. (2012). "Targeting the endocannabinoid system with cannabinoid
24 receptor agonists: pharmacological strategies and therapeutic possibilities."
25 *Philosophical Transactions of the Royal Society B: Biological Sciences* 367(1607):
26 3353-3363.
- 27 Robertson, N., A. Jazayeri, J. Errey, A. Baig, E. Hurrell, A. Zhukov, C. J. Langmead,
28 M. Weir and F. H. Marshall (2011). "The properties of thermostabilised G protein-
29 coupled receptors (StaRs) and their use in drug discovery." *Neuropharmacology*
30 60(1): 36-44.
- 31 Serrano-Vega, M. J., F. Magnani, Y. Shibata and C. G. Tate (2008). "Conformational
32 thermostabilization of the beta1-adrenergic receptor in a detergent-resistant form."
33 *Proc Natl Acad Sci U S A* 105(3): 877-882.
- 34 Sykes, D. A., C. Parry, J. Reilly, P. Wright, R. A. Fairhurst and S. J. Charlton (2014).
35 "Observed drug-receptor association rates are governed by membrane affinity: the
36 importance of establishing "micro-pharmacokinetic/pharmacodynamic relationships"
37 at the beta2-adrenoceptor." *Mol Pharmacol* 85(4): 608-617.

- 1 Tate, C. G. (2010). Practical considerations of membrane protein instability during
2 purification and crystallisation. *Heterologous Expression of Membrane Proteins*,
3 Springer: 187-203.
- 4 Tippett, D., B. Hoare, T. Miljus, D. A. Sykes and D. Veprintsev (2020). "ThermoFRET:
5 A novel nanoscale G protein coupled receptor thermostability assay functional in crude
6 solubilised membrane preparations." *BioRxiv*.
- 7 Vuckovic, Z. (2017). Development of a strategy for structural determination of $\alpha 2C$ and
8 $\beta 3$ adrenergic receptors. Ph.D., ETH Zurich.
- 9 Vukoti, K., T. Kimura, L. Macke, K. Gawrisch and A. Yeliseev (2012). "Stabilization of
10 functional recombinant cannabinoid receptor CB2 in detergent micelles and lipid
11 bilayers." *Plos one* 7(10).
- 12 Wacker, D., G. Fenalti, M. A. Brown, V. Katritch, R. Abagyan, V. Cherezov and R. C.
13 Stevens (2010). "Conserved binding mode of human beta2 adrenergic receptor
14 inverse agonists and antagonist revealed by X-ray crystallography." *J Am Chem Soc*
15 132(33): 11443-11445.
- 16 Wang, J.-H., X.-X. Shao, M.-J. Hu, D. Wei, W.-H. Nie, Y.-L. Liu, Z.-G. Xu and Z.-Y.
17 Guo (2017). "Rapid preparation of bioluminescent tracers for relaxin family peptides
18 using sortase-catalysed ligation." *Amino Acids* 49(9): 1611-1617.
- 19 White, C. W., E. K. Johnstone, H. B. See and K. D. Pflieger (2019). "NanoBRET ligand
20 binding at a GPCR under endogenous promotion facilitated by CRISPR/Cas9 genome
21 editing." *Cellular signalling* 54: 27-34.
- 22 Wouters, S. F. A., W. J. P. Vugs, R. Arts, N. M. de Leeuw, R. W. H. Teeuwen and M.
23 Merkx (2020). "Bioluminescent Antibodies through Photoconjugation of Protein G–
24 Luciferase Fusion Proteins." *Bioconjugate Chemistry* 31(3): 656-662.
- 25 Zhang, X., R. C. Stevens and F. Xu (2015). "The importance of ligands for G protein-
26 coupled receptor stability." *Trends in biochemical sciences* 40(2): 79-87.
- 27
- 28
- 29
- 30
- 31
- 32



1

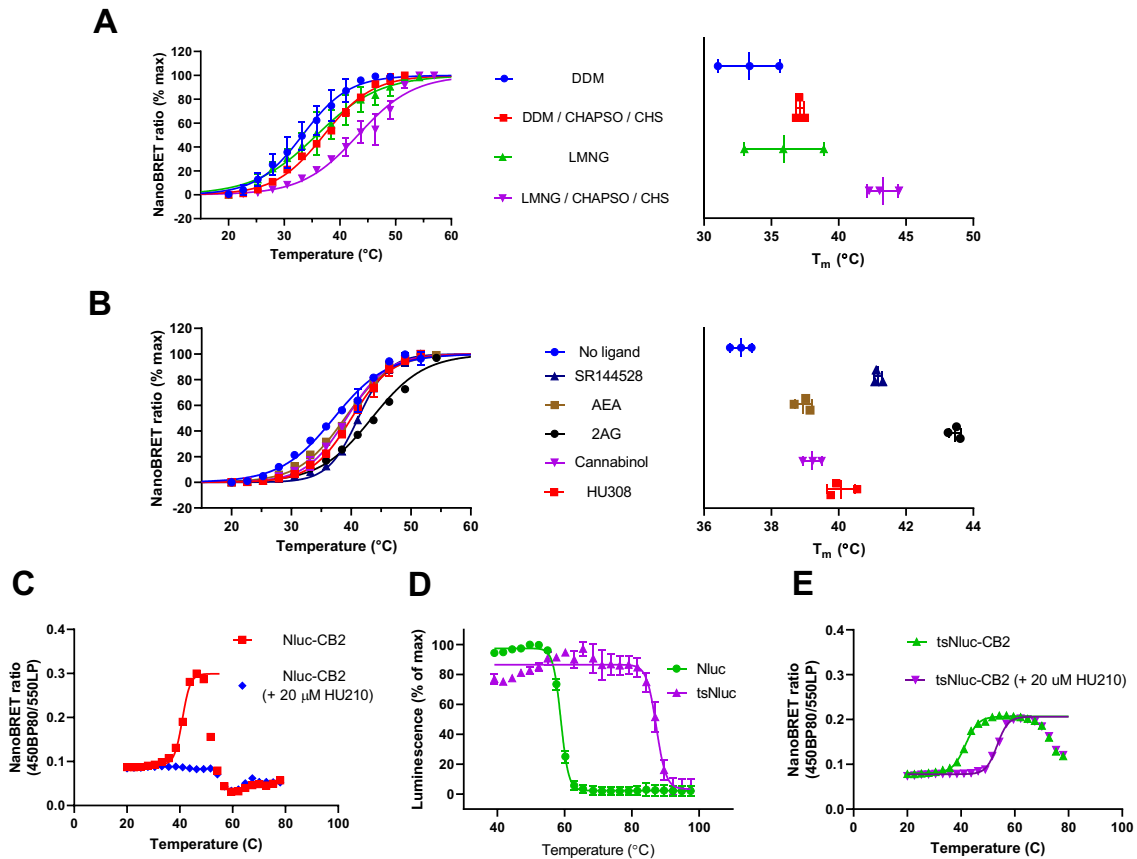
2 **Figure 1: Principle of ThermoBRET assay measured in 384-well plate format.**

3 Detergent solubilised non-purified membrane preparations expressing GPCRs fused
4 at the N-terminus with Nluc (or tsNluc) are heated using a PCR thermocycler in the
5 presence of sulfo-Cy3 maleimide (SCM). As the protein unfolds due to thermal
6 denaturation, SCM reacts with newly exposed cysteine residues putting the sulfo-Cy3
7 acceptor fluorophore in proximity with the Nluc donor. At higher temperatures, protein
8 aggregation leads to a decrease in the NanoBRET signal and these points are
9 truncated before fitting to a Boltzmann sigmoidal equation to obtain a melting point
10 (T_m).

11

12

13

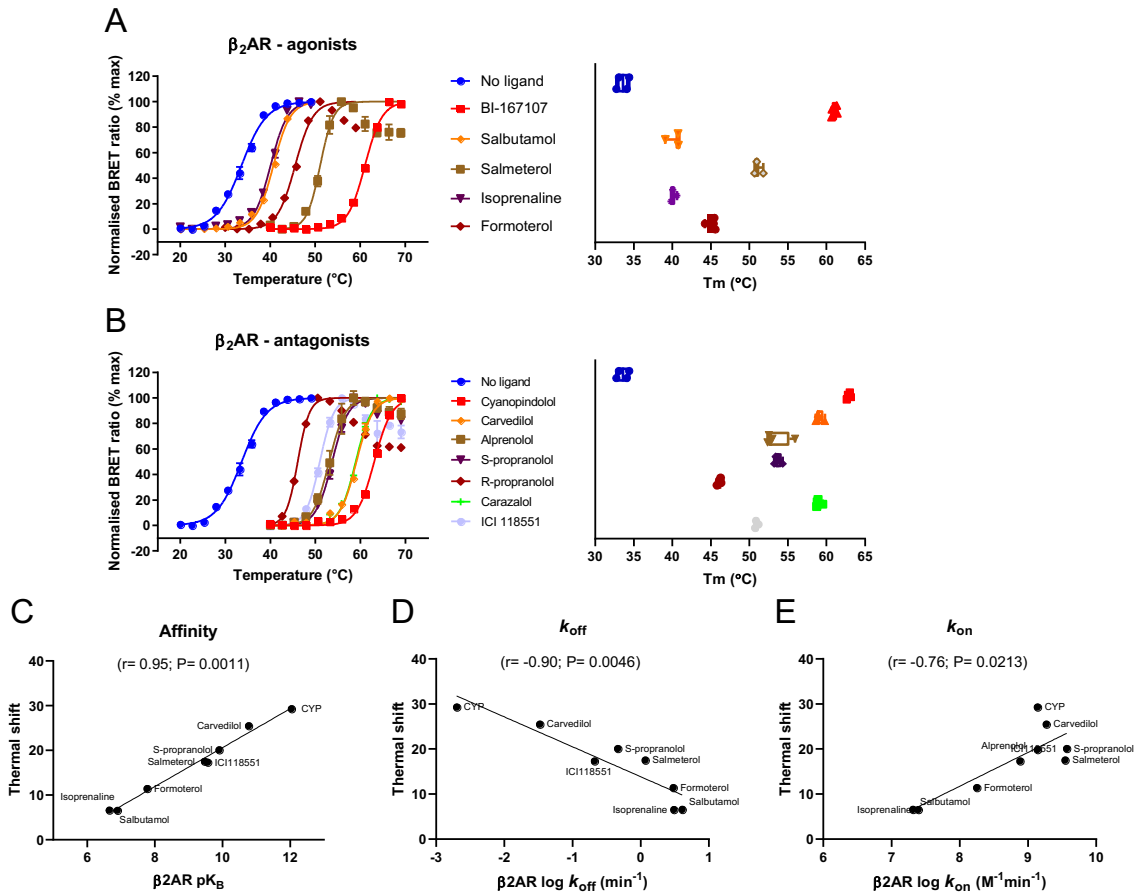


1

2 **Figure 2: ThermoBRET measurements in different detergent conditions and with**
 3 **stabilising ligands, demonstrating superior performance of tsNluc over Nluc for**
 4 **high thermostability situations.** ThermoBRET thermostability curves and pooled T_m
 5 measurements for **(A)** Nluc-CB₂ solubilised in the indicated detergent conditions. **(B)**
 6 in DDM/CHAPSO/CHS, in the presence/absence of ligands. **(C)** ThermoBRET curve
 7 for Nluc-CB₂ solubilised in DDM/CHAPSO/CHS, showing that the curve for the
 8 receptor bound to HU210 cannot be fitted as it is stable beyond the point of Nluc
 9 stability. **(D)** Luminescence thermostability curves of purified Nluc and tsNluc. **(E)**
 10 ThermoBRET using tsNluc-CB₂ in the presence/absence of HU210, showing a full fit
 11 for both curves. **(A)** and **(B)** show pooled normalised data showing mean \pm standard
 12 deviation for the number of experimental replicates evident in the far-right graph ($n \geq 2$).
 13 **(C)** and **(E)** are raw fitted data from a single experiment performed 3 times. **(D)** is
 14 pooled normalised data from 3-independent experiments.

15

16



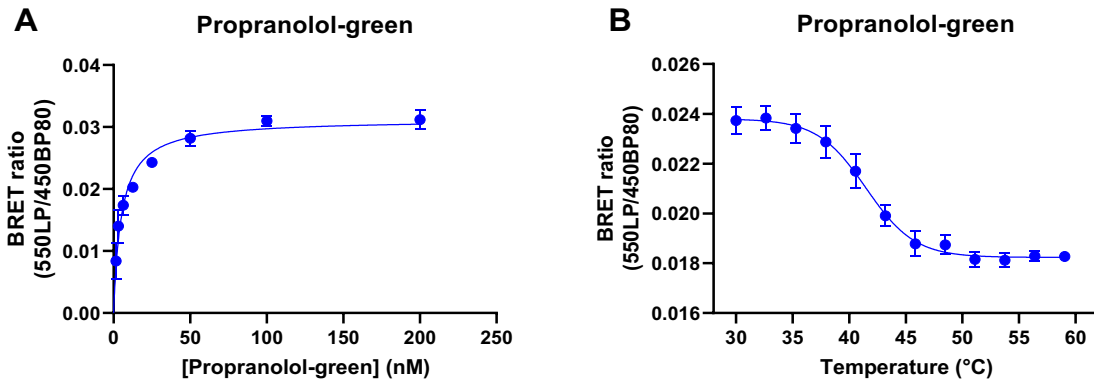
1

2

3 **Figure 3: tsNluc β_2 AR thermoBRET measurements in 0.1% DDM with stabilising**
 4 **ligands and high thermostability situation.** ThermoBRET thermostability curves
 5 and pooled T_m measurements for tsNluc- β_2 AR solubilised in DDM in the
 6 presence/absence of **(A)** agonist ligands and **(B)** antagonist ligands. The magnitude
 7 of shifts are shown on panels on the right, with ligands as indicated on the left panel.
 8 Correlations of ligand thermostability (ΔT_m) with **(C)** ligand affinity, **(D)** ligand k_{off} and
 9 **(E)** ligand k_{on} . **(A)** and **(B)** show pooled normalised data showing mean \pm standard
 10 deviation for the number of experimental replicates evident in the far-right graph ($n \geq 3$),
 11 pooled normalised data from 3 or more independent experiments. Radioligand binding
 12 data values were taken from (Sykes, Parry et al. 2014).

13

14



1

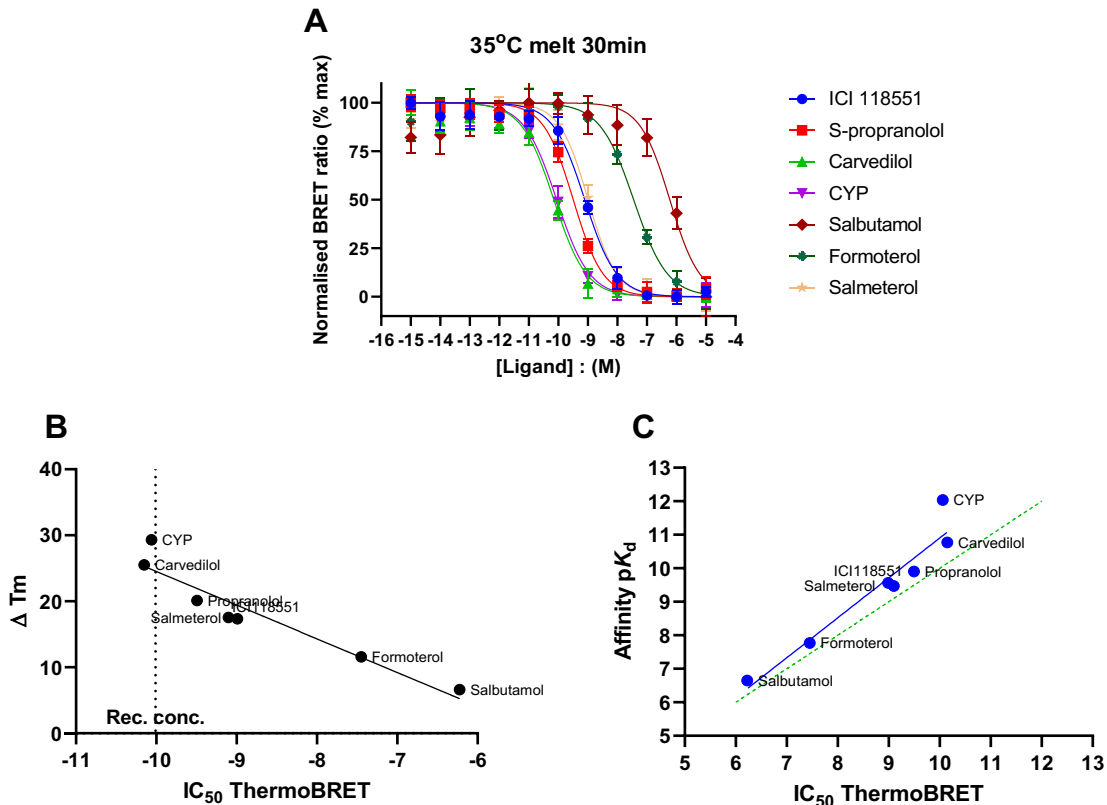
2 **Figure 4: BRET based fluorescent tracer binding to the β_2 AR solubilised in DDM.**

3 (A) Saturation binding curve of propranolol-green binding the β_2 AR. ThermoBRET

4 thermostability curve for tsNluc- β_2 AR in the presence of (1 μ M) propranolol-green.

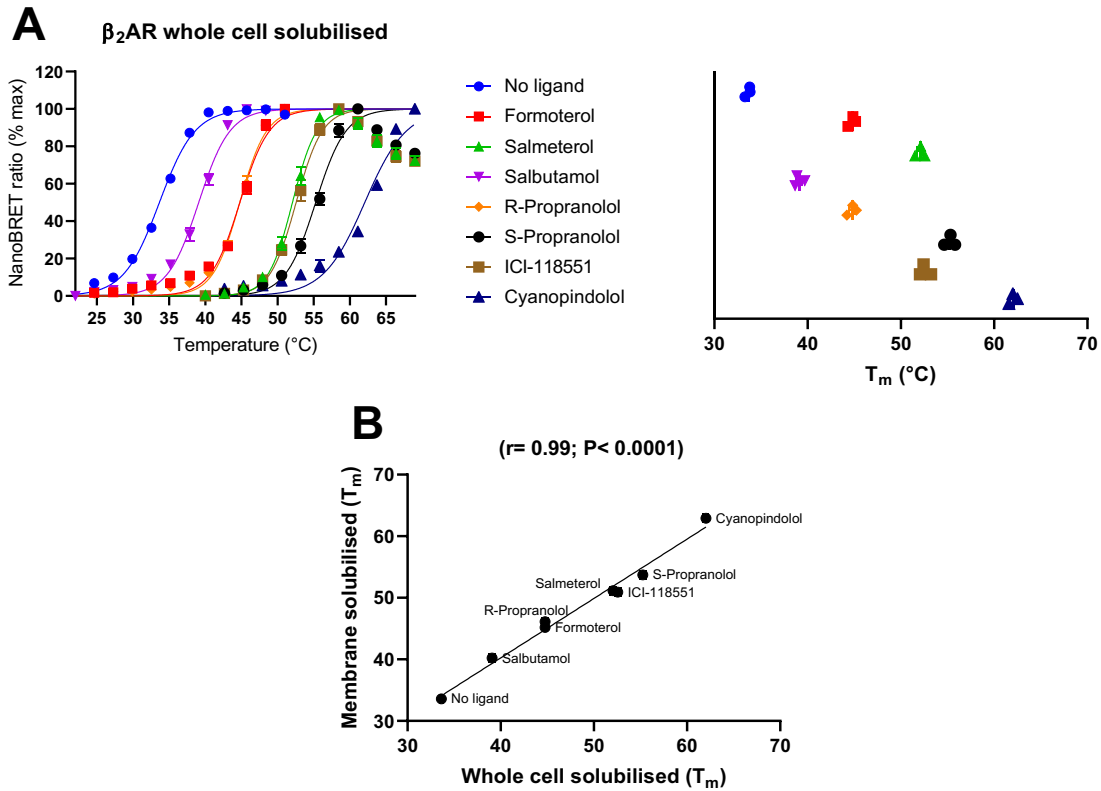
5 Data is plotted as the mean \pm standard error for 3 replicates.

6



1
2
3
4
5
6
7
8
9
10
11
12

Figure 5: tsNluc β_2 AR thermoBRET measurements in 0.1% DDM with stabilising ligands expressed as a function of concentration. (A) ThermoBRET IC_{50} curves obtained at a fixed temperature of 35°C following a 30min incubation with either agonists or antagonist ligands. Normalised data is plotted as the mean \pm standard deviation for 3 replicates. ThermoBRET IC_{50} values were derived for this smaller test set and correlated with **(B)** the change in thermal shift obtained at fixed concentrations of individual agonist or antagonist and **(C)** radioligand binding derived ligand affinity values. All correlations are derived from mean thermostability measurements consisting of at least 3 replicates. Radioligand binding data values were taken from (Sykes, Parry et al. 2014).

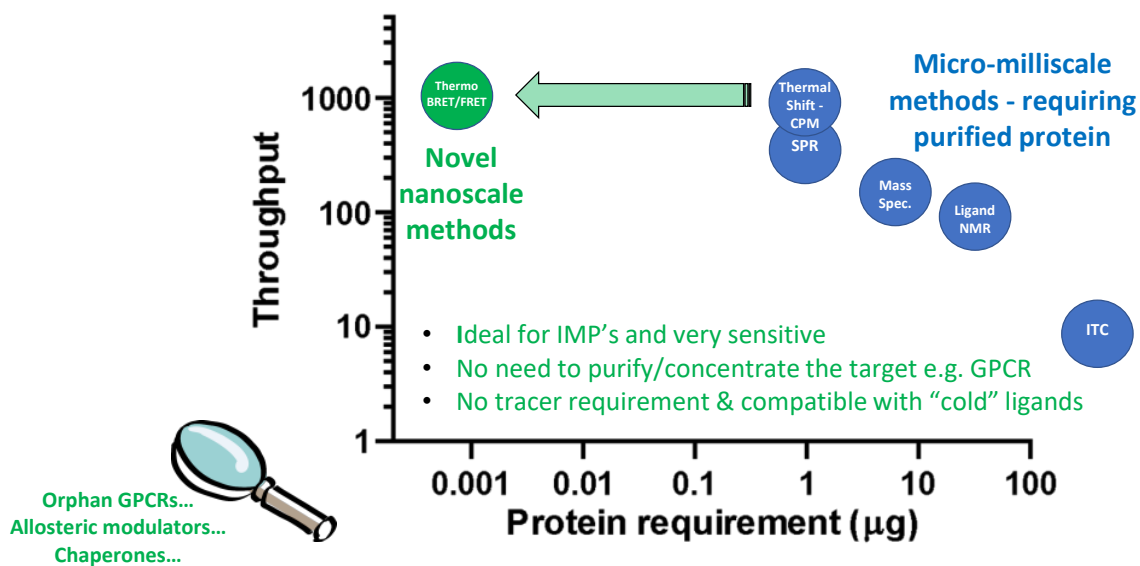


1

2 **Figure 6: tsNluc β_2 AR thermoBRET measurements in 0.1% DDM following**
3 **solubilisation from whole cells.** ThermoBRET thermostability curves and pooled T_m
4 measurements for tsNluc- β_2 AR solubilised in DDM in the presence/absence of (A)
5 agonist ligands and antagonist ligands. The magnitude of shifts is shown on the panel
6 on the right (B) shows the correlation between T_m 's determined following solubilisation
7 of the β_2 AR from HEK293TR membranes or whole cells. (A) and (B) show pooled
8 normalised data showing mean \pm standard deviation for the number of experimental
9 replicates evident in the far-right graph ($n \geq 3$), pooled normalised data from 3 or more
10 independent experiments.

11

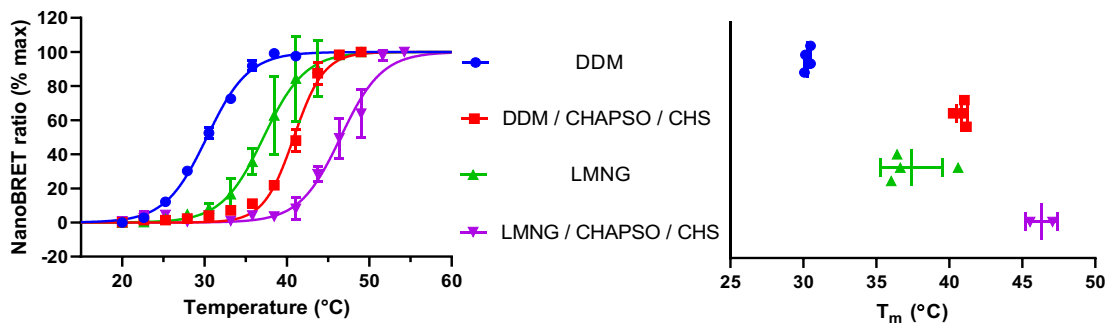
12



1

2 **Figure 7: A comparison of biophysical techniques used in drug screening**
3 **cascades.** Outlined are the protein requirements of each technique and their
4 estimated daily throughput screening potential, along with the advantages of
5 ThermoBRET and some potential uses.

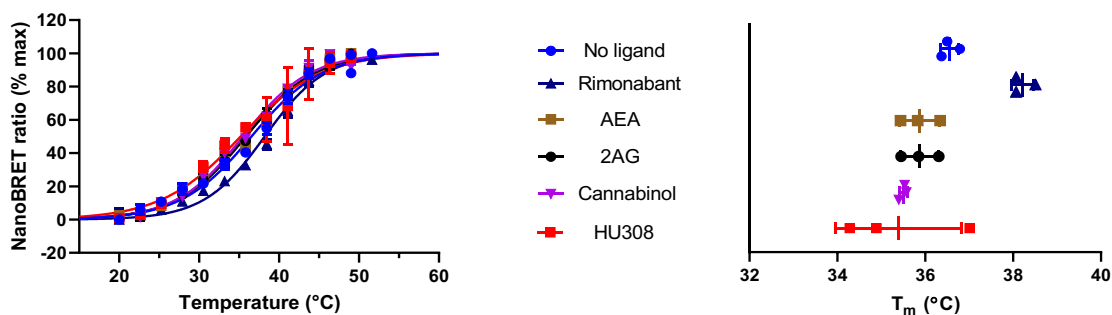
6



1

2 **Supplementary Figure 1: Nluc-β₂AR thermostability in different detergent**
3 **conditions.** Data are pooled normalised values showing the mean ± standard
4 deviation for the number of experimental replicates evident in the far-right graph (n≥2).

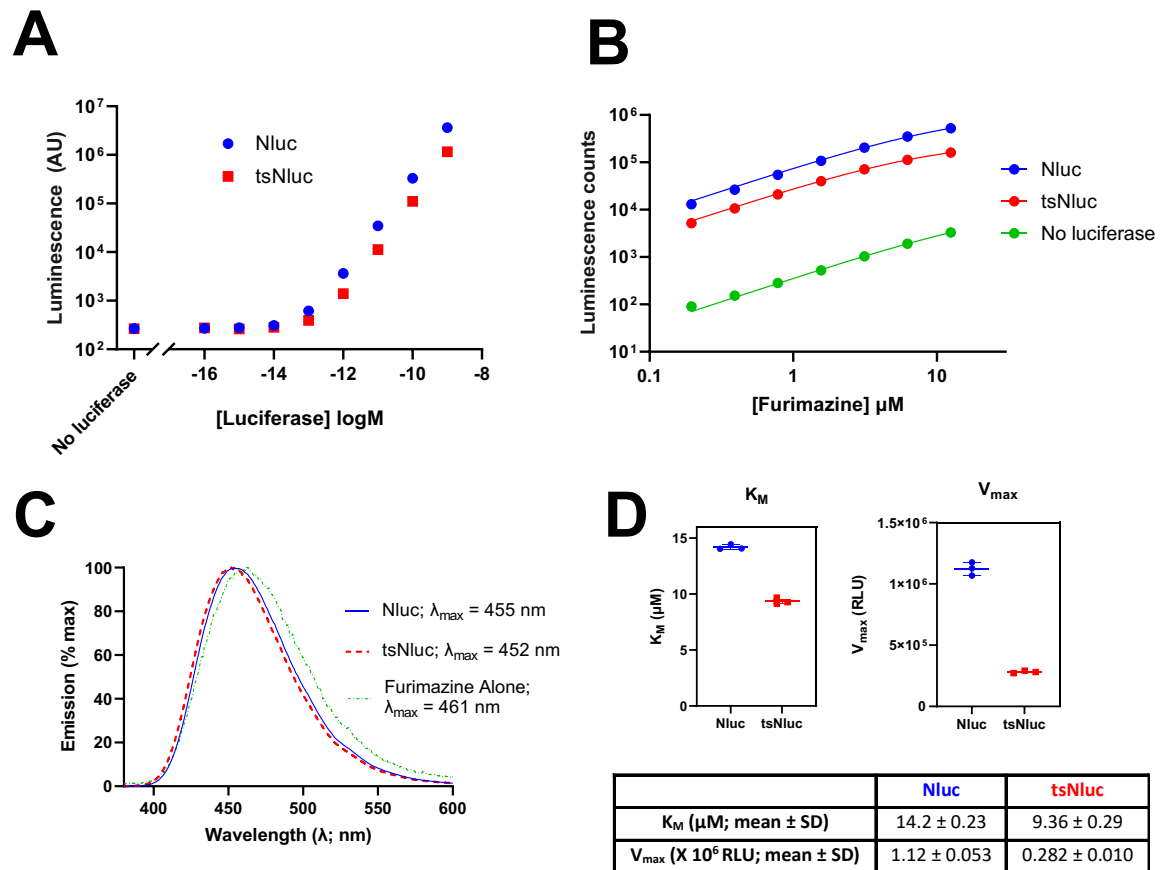
5



1
2

3 **Supplementary Figure 2: Thermostability of Nluc-CB₁(91-472) solubilised in**
4 **DDM/CHAPSO/CHS.** Data are pooled normalised values showing the mean \pm
5 standard deviation for the number of experimental replicates evident in the far-right
6 graph ($n \geq 3$). All ligands were present at a concentration of 20 μ M.

7
8



1

2 **Supplementary Figure 3: Characterisation of purified Nluc and tsNluc. (A)**

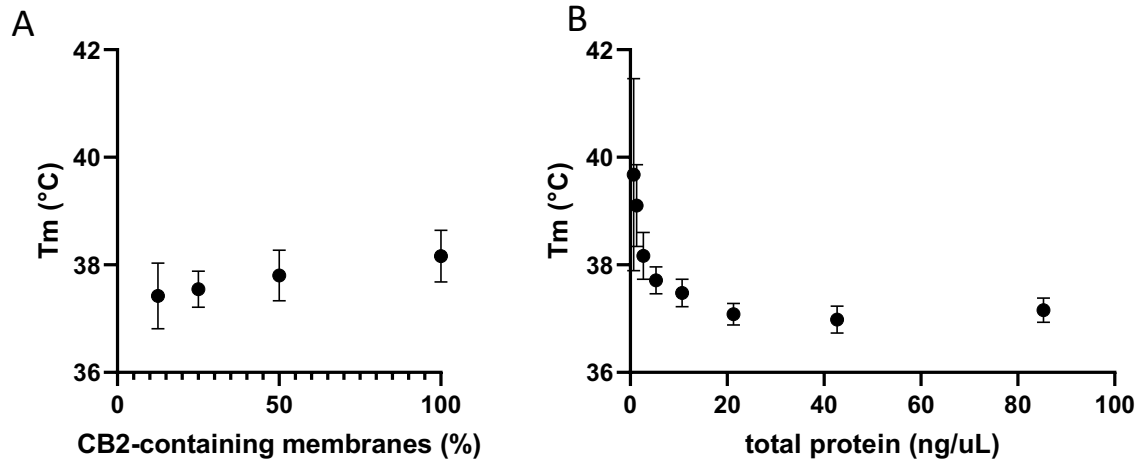
3 Different concentrations of luciferase proteins were mixed with 10 μM furimazine in a
4 white 384-well optiplate and luminescence was measured with PHERAstar FSX
5 plate reader with gain set to 2000 and 0.5 second measurement interval time. **(B)**

6 Different concentrations of furimazine were mixed with 10 pM of purified luciferase
7 and luminescence was measured with PHERAstar FSX plate reader with gain set to
8 3000 and 0.5 second measurement interval time. Data was fitted to a Michealis-

9 Menten equation in GraphPad Prism to derive K_M and V_{max} values for Nluc and

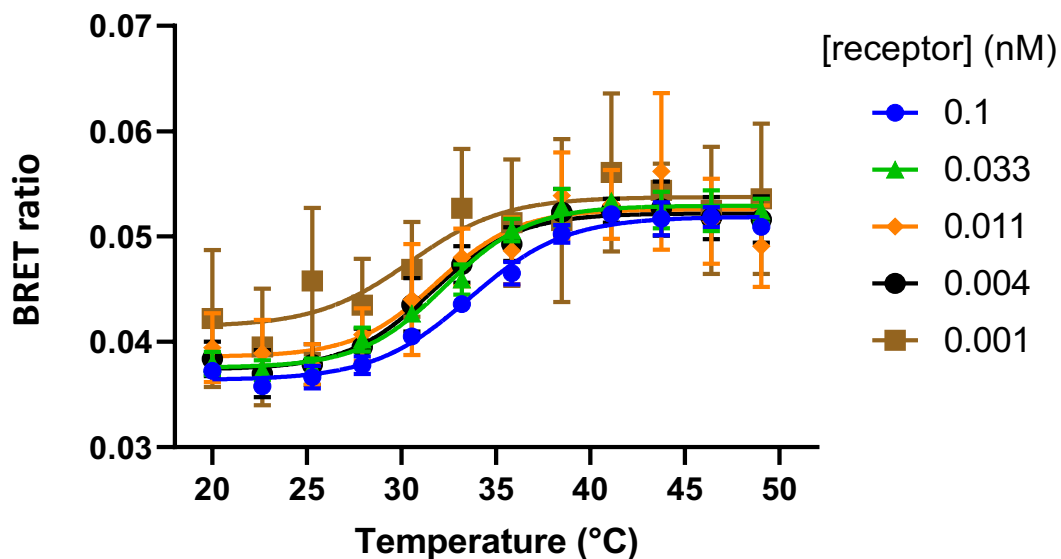
10 tsNluc. **(C)** Spectral scan of luminescence emission from 10 μM furimazine in the
11 presence of absence of purified luciferases. **(D)** K_M and V_{max} determinations from **(B)**.

12 Data points and error bars represent the mean \pm SD of 3 independent experiments
13 performed in duplicate. Experiments were performed in CORE buffer at an ambient
14 room temperature (26 - 27 $^\circ\text{C}$ at that time of year).



1
2
3
4
5
6
7
8
9
10
11
12
13

Supplementary Figure 4: Dependence of T_m values on CB2 and membrane concentration (expressed as total protein). (A) T_m values for CB2-containing HEK2993 membranes mixed in different ratios with "empty" non-transfected HEK2993 membranes to a total of 26 ng/ μ L of protein. (B) T_m values for 0.67 ng/ μ L CB2-containing HEK2993 membranes mixed with increasing concentrations of non-transfected HEK2993 membranes. Samples were melted for 5 min at a temperature gradient 20-52°C in the presence of 0.1% DDM/0.05% CHAPSO/0.03% CHS. N=3, error bars are SEM.



1

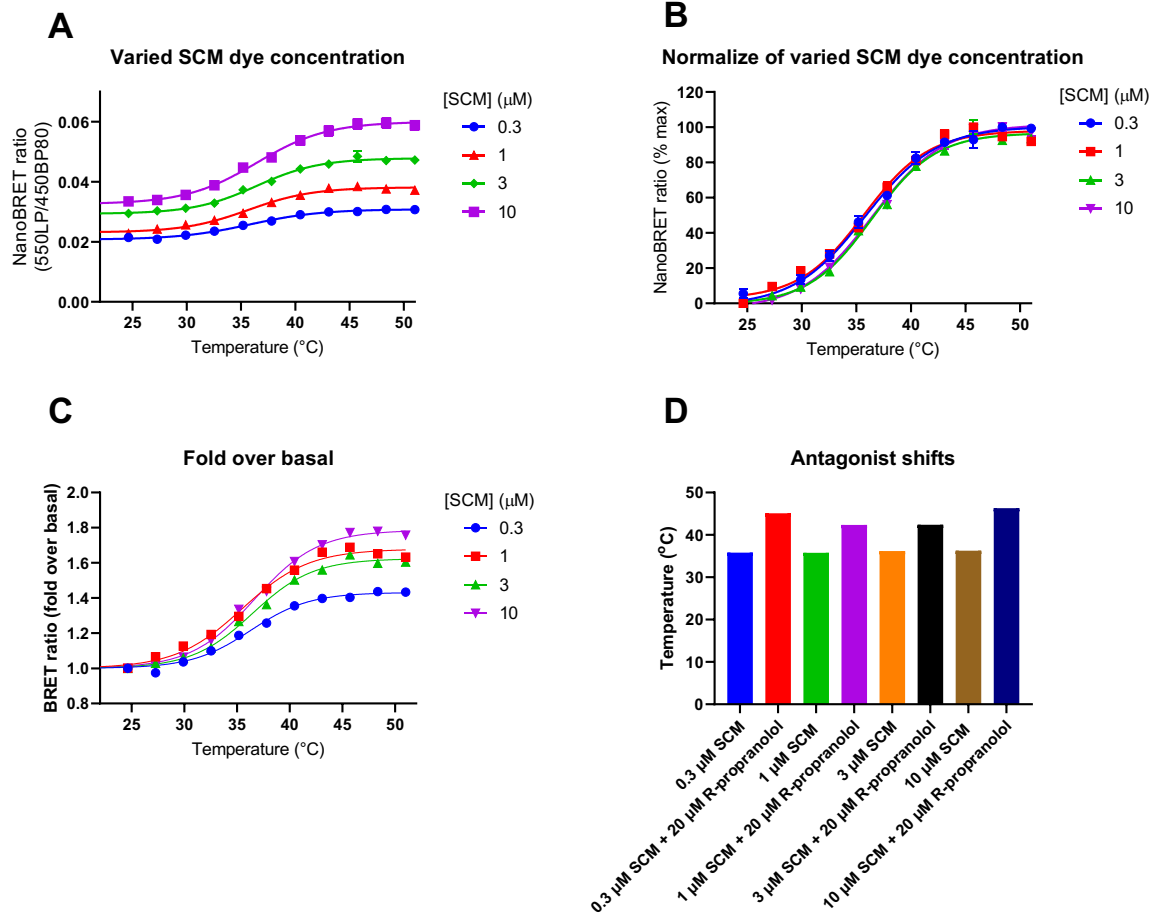
2 **Supplementary Figure 5: Assay sensitivity as determined by assessing the**
3 **Thermostability of different concentrations of tsNluc-β₂AR solubilised in DDM.**

4 Data are pooled normalised values showing the mean ± standard deviation. The
5 different concentrations of receptor were estimated by diluting tsNluc and determining
6 the level of luminescence at a fixed concentration of furimazine and comparing it to
7 the levels of luminescence observed following dilution of the solubilised receptor.

8

9

10



1
2 **Supplementary Figure 6: Effect of different SCM dye concentrations on T_m**
3 **determinations from the tsNluc- β_2 AR solubilised in DDM.** Increasing
4 concentrations of SCM dye were incubated with a fixed level of tsNluc- β_2 AR and
5 subject to a thermal gradient, T_m values were determined following the addition of a
6 fixed concentration of furimazine (10 μM). BRET ratio values are shown in (A) and
7 normalised data in (B) for the different dye concentrations. Fold over basal values are
8 shown in (C), and demonstrate the potential for signal improvement when increasing
9 SCM concentration from 0.3 to 10 μM. The effect of dye concentration on the
10 antagonist shift observed is shown in (D). Data are single values determined from a
11 single experiment.

12
13

1 **Supplementary Information 1: Amino acid sequences of expression constructs**
2 **used in this study.**

3

4 **> pcDNA4/TO SigPep-TwinStrep-Nluc-CB₂**

5 MRLCIPQVLLALFLSMLTGPGEASDIDGAPAFKSVQTGEFTAAGSAW**SHHPQFEK**
6 GGGSGGGSGGSAW**SHHPQFEK**GSGGSEDLMVFTLEDFVGDWRQTAGYNLDQVLE
7 QGGVSSLFQNLGVSVTPIQRIVLSGENGLKIDIHVIIPYEGLSGDQMGQIEKIFKVYYP
8 VDDHHFKVILHYGTLVIDGVTPNMIDYFGRPYEGIAVFDGKKITVTGTLWNGNKIIDE
9 RLINPDGSLLFRVTINGVTGWRLCERILAPAGTMEECWVTEIANGSKDGLDSNPMK
10 DYMILSGPQKTAVAVLCTLLGLLSALENAVLYLILSSHQLRRKPSYLFIGSLAGADF
11 LASVVFACSFVNFHVFHGVDSKAVFLLKIGSVTMTFTASVGSLLLTAIDRYLCLRYPP
12 SYKALLTRGRALVTLGIMWVLSALVSYLPLMGWTCPCPRPCSELFPLIPNDYLLSWLL
13 FIAFLFSGIITYGHVWLKAHQHVASLSGHQDRQVPGMARMRLDVRLAKTLGLVLA
14 VLLICWFPVLALMAHSLATLSDQVKKAFACSMCLCLNSMVNPVIYALRSGEIRSSA
15 HHCLAHWKKCVRGLGSEAKEEAPRSSVTETeadgKITPWPDSRDLDLSDC*

16 **> pcDNA4/TO SigPep-TwinStrep-Nluc-β₂AR**

17 MRLCIPQVLLALFLSMLTGPGEASDIDGAPAFKSVQTGEFTAAGSAW**SHHPQFEK**
18 GGGSGGGSGGSAW**SHHPQFEK**GSGGSEDLMVFTLEDFVGDWRQTAGYNLDQVLE
19 QGGVSSLFQNLGVSVTPIQRIVLSGENGLKIDIHVIIPYEGLSGDQMGQIEKIFKVYYP
20 VDDHHFKVILHYGTLVIDGVTPNMIDYFGRPYEGIAVFDGKKITVTGTLWNGNKIIDE
21 RLINPDGSLLFRVTINGVTGWRLCERILAPAGTMGQPGNGSAFLLAPNGSHAPDHD
22 VTQQRDEVWVGMGIVMSLIVLAIVFGNVLVITAIKFERLQTVTNYFITSLACADLV
23 MGLAVVPFGAAHILMKMWTFGNFWCFWTSIDVLCVTASIELCVIAVDRYFAITSP
24 FKYQSLLTKNKARVILMVWIVSGLTSFLPIQMHWRATHQEAINCYANETCCDFFT
25 NQAYAIASSIVSFYVPLVIMVFVYSRVFQEAQRQLQKIDKSEGRFHVQNLSQVEQDG
26 RTGHGLRRSSKFCLKEHKALKTLGIIMGTFTLCWLPFFIVNIVHVIQDNLIRKEVYILLN
27 WIGYVNSGFNPLIYCRSPDFRIAFQELLCLRSSLKAYGNGYSSNGNTGEQSGYHV
28 EQEKENKLLCEDLPGTEDFVGHQGTVPSDNIDSQGRNCSTNDSLL*

29 **> pcDNA4/TO SigPep-TwinStrep-Nluc-CB₁(91-472)[#]**

30 MRLCIPQVLLALFLSMLTGPGEASDIDGAPAFKSVQTGEFTAAGSAW**SHHPQFEK**
31 GGGSGGGSGGSAW**SHHPQFEK**GSGGSEDLMVFTLEDFVGDWRQTAGYNLDQVLE
32 QGGVSSLFQNLGVSVTPIQRIVLSGENGLKIDIHVIIPYEGLSGDQMGQIEKIFKVYYP
33 VDDHHFKVILHYGTLVIDGVTPNMIDYFGRPYEGIAVFDGKKITVTGTLWNGNKIIDE
34 RLINPDGSLLFRVTINGVTGWRLCERILAPAGTENEENIQCGENFMDIECFMVLNPS
35 QQLAIAVLSLTLGFTVLENLLVLCVILHSRSLRCRPSYHFIGSLAVADLLGSVIFVYS
36 FIDFHV FHRKDSRNVFLFKLGGVTASFTASVGSFLT AIDRYIS IHRPLAYKRIVTRPK
37 AVVAFCLMWTIAIVAVLPLLGNCEKLQSVCSDFPHIDETYLFWIGVTSVLLLFIW
38 YAYMYILWKAHSHAVRMIQRGTQKSIIIHTSEDGKVQVTRPDQARMDIRLAKTLVLIL
39 VVLIICWGPLLAIMVYDVF GKMNKLIKTVFAFCSMLCLLNSTVNPIIYALRSKDLRHAF
40 RSMFPSCEGTAQPLDNSMGDSCLHKHANNAASVHRAAESCICKSTVKIAKVTMSV
41 STDTSAEAL*

1 #The full-length CB₁ receptor contains an unusually long (around 117 amino acids)
2 and likely unstructured N-terminal domain. It was therefore truncated at the N-terminus
3 in order to bring the Nluc tag in proximity with the transmembrane helices.

4 > **pcDNA4/TO SigPep-TwinStrep-tsNluc-CB₂**

5 MRLCIPQVLLALFLSMLTGPGEGSASDIGAPAFKSVQTGEFTAAGSAW**SH**PQ**FEK**
6 GGGSGGGSGGSAW**SH**PQ**FEK**GSGGSEDLMVFTLEDFVGDWEQTAAYNLDQVLE
7 QGGVSSLLQNLAVSVTPIQRIVRSGENALKIDIHVIIPYEGLSADQMAQIEEVFKVVYP
8 VDDHHFKVILPYGTLVIDGVTPNMLNYFGRPYEGIAVFDGKKITVTGTLWNGNKIIDE
9 RLITPDGSMLFRVTINGVSGWRLFKKIS**PAGTMEECWVTEIANGSKDGLDSNPMKD**
10 YMILSGPQKTAVAVLCTLLGLLSALENVAVLYLILSSHQLRRKPSYLFIGSLAGADFLA
11 SVVFACSFVNFHFVHGVDSKAVFLKIGSVTMTFTASVGSLLLTAIDRYLCLRYPPSY
12 KALLTRGRALVTLGIMWVLSALVSYLPLMGWTCPCPRPCSELFPLIPNDYLLSWLLFI
13 AFLFSGIITYGHVLWKAHQHVASLSGHQDRQVPGMARMRLDVR**LAKTLGLVLAVL**
14 LICWFPVLALMAHSLATTLSDQVKKAF**AFCSMLCLINSMVNPVIYALRSGEIRSSAHH**
15 CLAHWKKCVRGLGSEAKEEAPRSSVTET**EADGKITPWPDSRDLDLSDC***

16 > **pJ411 His-TEV-Nluc**

17 MKKHHHHHHHHHH**ENLYFQGG**SVFTLEDFVGDWRQTAGYNLDQVLEQGGVSSLF
18 QNLGVS**VTPIQRIVLSGEN**LKIDIHVIIPYEGLSGDQMGQIEKIFKVVYPVDDHHFKV
19 ILHYGTLVIDGVTPNMIDYFGRPYEGIAVFDGKKITVTGTLWNGNKIIDERLINPDGSL
20 LFRV**TINGVTGWRLCERILA***

21 > **pJ411 HIS-TEV-TsNluc**

22 MKKHHHHHHHHHH**ENLYFQGG**SVFTLEDFVGDWEQTAAYNLDQVLEQGGVSSLL
23 QNLAVSVTPIQRIVRSGENALKIDIHVIIPYEGLSADQMAQIEEVFKVVYPVDDHHFKV
24 ILPYGTLVIDGVTPNMLNYFGRPYEGIAVFDGKKITVTGTLWNGNKIIDERLITPDGS
25 MLFRV**TINGVSGWRLFKKIS***

26

